

Electronic Supplementary Information

Porous single-crystalline palladium nanoflowers with enriched {100} facets for highly enhanced ethanol oxidation

Kun Qi, Qiyu Wang, Weitao Zheng,* Wei Zhang and Xiaoqiang Cui*

Department of Materials Science, Key Laboratory of Automobile Materials of MOE and State Key Laboratory of Superhard Materials, Jilin University, Changchun 130012, Jilin, People's Republic of China.

E-mail: xqcui@jlu.edu.cn (X. Q. Cui); wtzheng@jlu.edu.cn (W. T. Zheng)

Contents:

Figure. S1 TEM, HRTEM and SAED of Pd nanocube seeds

Figure. S2 EDX and XPS data of Pd PSNFs

Figure. S3 HRTEM and FFT image of a randomly picked Pd PSNF

Figure. S4 Photograph of solution color change during the reaction

Figure. S5 TEM, HRTEM, and FFT patterns of Pd black

Figure. S6 Characterization of the cleaning process of Pd PSNFs

Figure. S7 Mass electrochemical active area (ECSA) of the catalysts

Figure. S8 Blank Cyclic voltammograms of Pd-based catalysts

Figure. S9 Amplified graph of onset-potential for Pd-based catalysts

Figure. S10 EOR specific activity cyclic voltammograms of Pd-based catalysts

Figure. S11 EOR cyclic voltammograms of three different size Pd PSNFs

Table. S1 ICP-MS data of Pd-based catalysts

Table. S2 Mass loading, geometric area, active surface area and electrochemical roughness of Pd-based catalysts

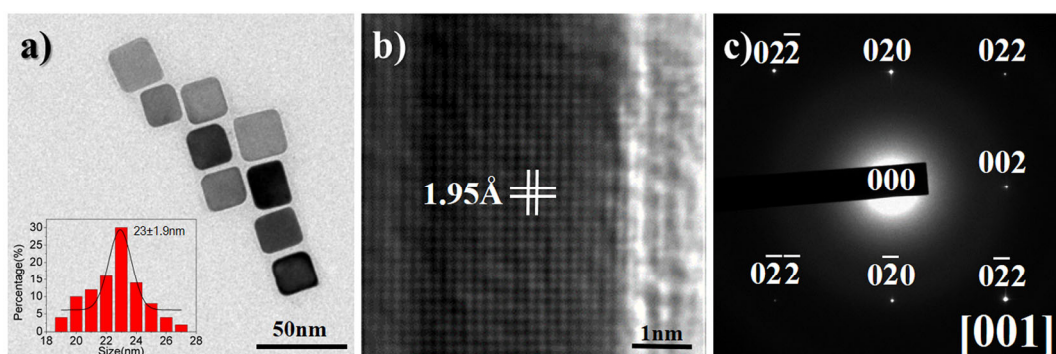


Fig. S1 (a) TEM image of single crystalline Pd nanocube seeds, inset shows the particle size distribution. (b) FFT contrast refined HRTEM image of a Pd nanocube seed. (c) SAED pattern of Pd nanocube seed recorded along the [001] zone axis.

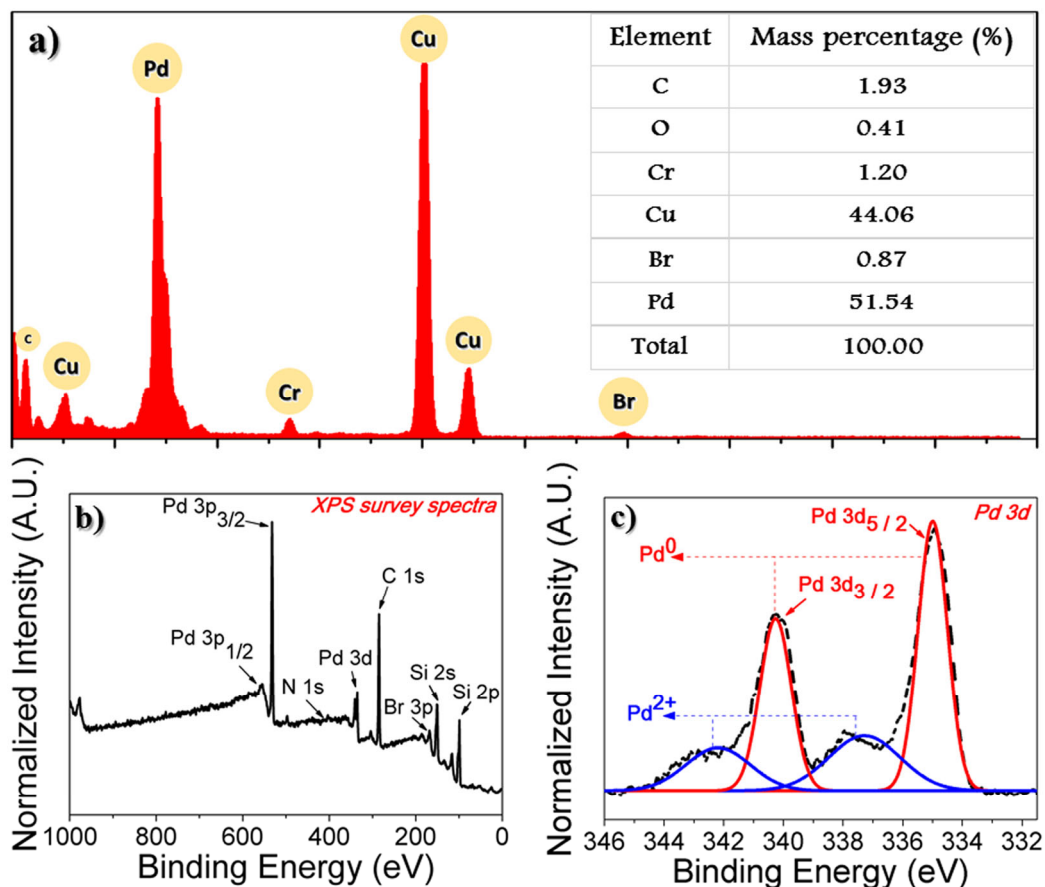


Fig. S2 Elemental and electronic state analysis of as-synthesized Pd PSNFs. (a) EDX spectrum of the Pd PSNFs. Inset shows the mass percentage of different elements (Trace amount of Cr is impurity on the sample stage, Br can be attribute to the capping agents on the PSNFs surface). (b) XPS survey spectra of Pd PSNFs (Elements of C and Br can be attribute to the capping agents on the PSNFs surface, Si comes form the Si wafer as the XPS substrate). (c) Pd 3d XPS spectra of the Pd PSNFs.

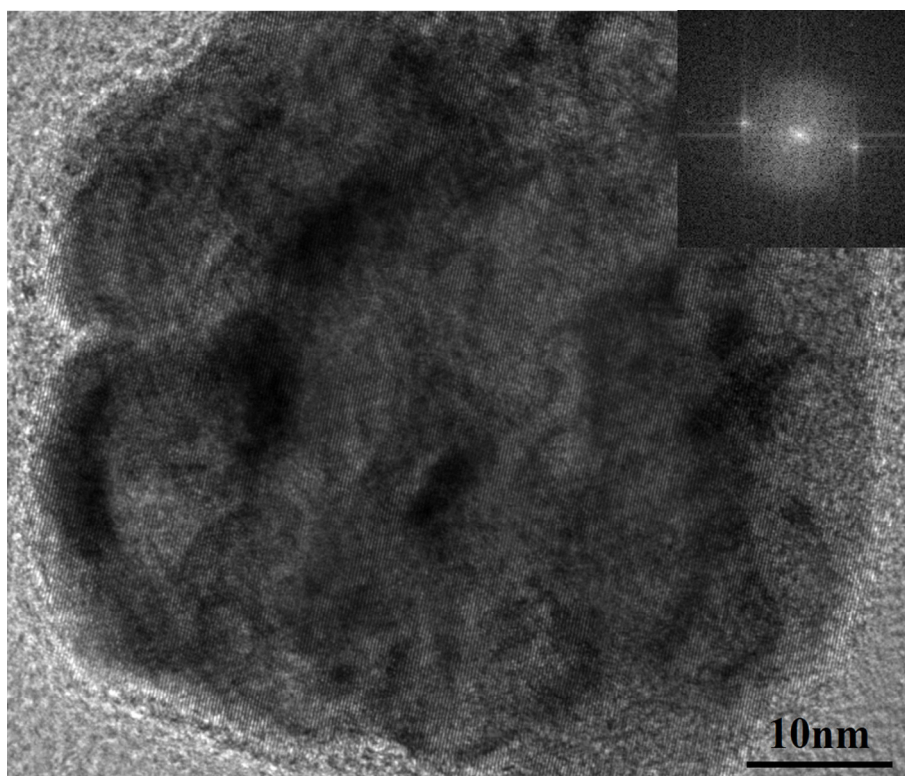


Fig. S3 HRTEM image of a randomly picked Pd PSNF, which clearly shows crystalline grains are arranged by the same orientation, indicating the single-crystalline nature of the nanoparticle; inset shows the FFT pattern of the entire nanoparticle.¹

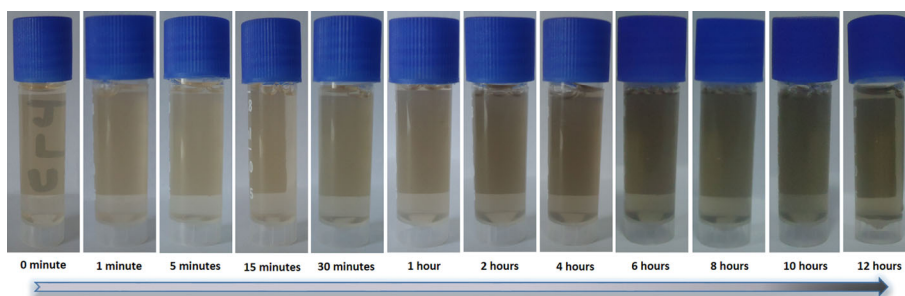


Fig. S4 Solution color change with the reaction proceeding from 0 minute to the termination (0 minute counts from the addition of ascorbic acid and stored at 40 °C without disturbance).

From 0-15 min, rarely change of the solution color was observed corresponding to the formation of small concave Pd nanocubes with the size increasing from 23 nm to about 35 nm. After 15 min, the color of the solution become darker, indicating the change of morphology and the increase of the particle size.

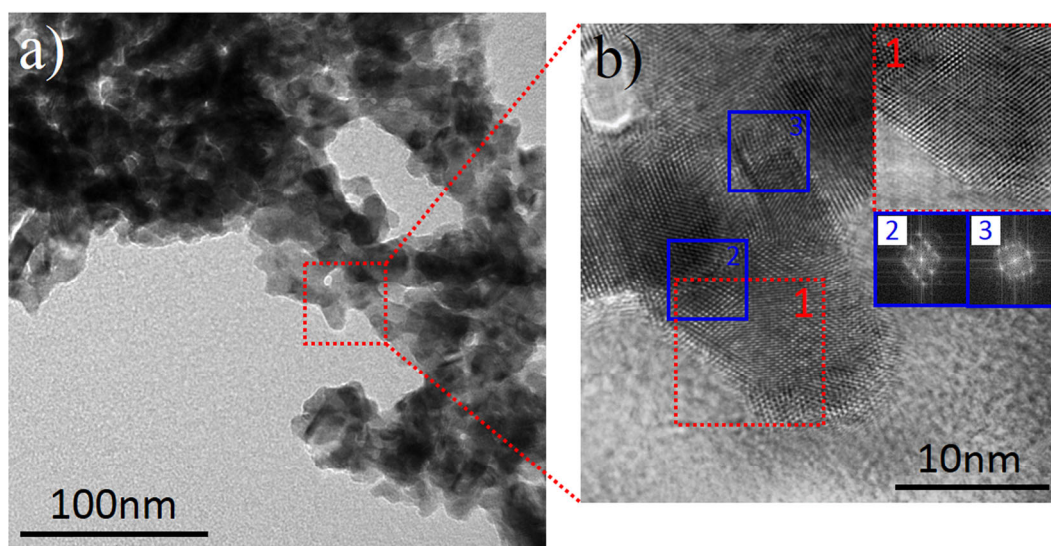


Fig. S5 (a) TEM image of Pd black (b) HRTEM image of Pd black takes from red dotted line box indicated in (a). Inset in (b) with red dotted line box shows FFT refined HRTEM image, which clearly reveals that there is no obvious high-index-facets in Pd black catalyst. Insets in (b) with blue solid line show the live FFT patterns of Pd black, which reveal the existence of lattice defects.

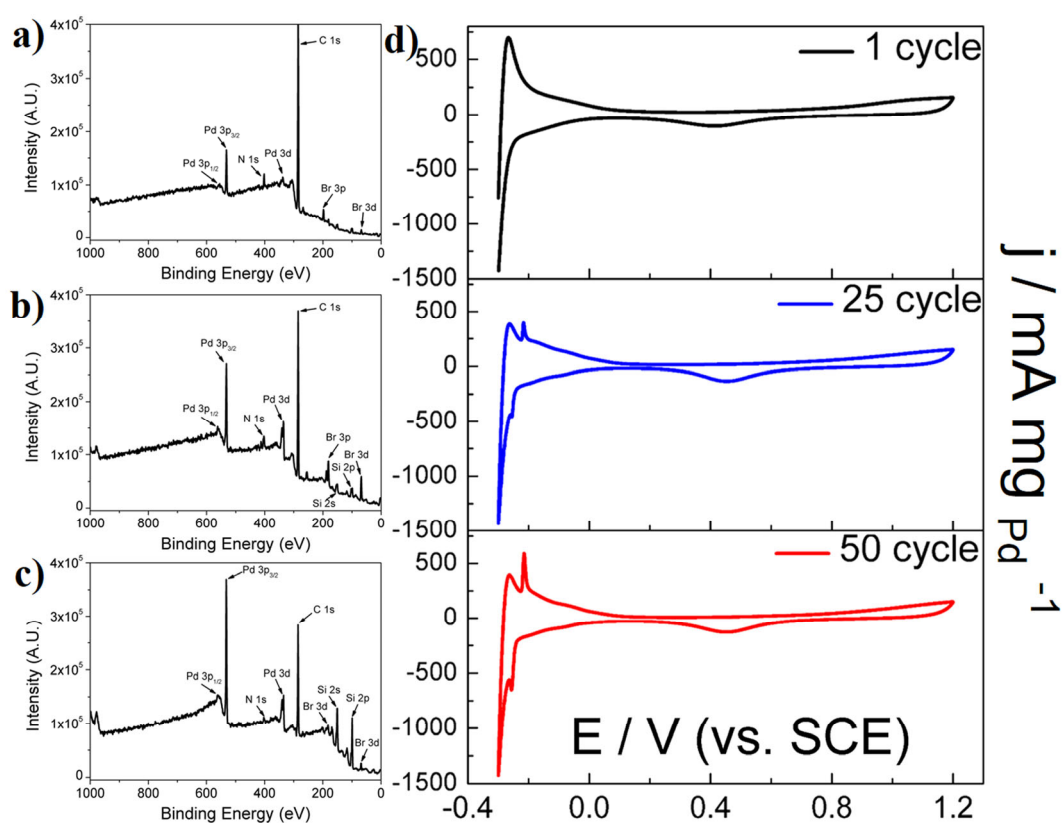


Fig. S6 Cleaning process of Pd PSNFs. (a) XPS survey spectra of Pd PSNFs before washing. (b) XPS survey spectra of Pd PSNFs after washing with deionized water for three times. (c) XPS survey spectra of Pd PSNFs after the electrochemical cleaning process. (d) Cyclic voltammograms of Pd PSNFs during electrochemical cleaning process in 0.5 M H₂SO₄ with a scan rate of 50 mV S⁻¹.

The influence of CTAB that may bind on the facets of Pd PSNFs is minimized by following steps: First of all, we washed the as-synthesized Pd PSNFs with 40 °C deionized water for three times to remove the excess CTAB in the solution and also on the nanoparticle's surface. As shown in Fig. S6a-S6b, the XPS survey spectra of Pd PSNFs after washing with deionized water for three times show a obvious decrease in peak intensity for element C, Br and increase for Pd that implies a preliminary cleaning. After cleaning with water washing, we applied a electrochemical cleaning process in a N₂ saturated 0.5 M H₂SO₄ solution by performing cyclic voltammetry scanning at -0.3–1.2 V for 50 cycles until stable voltammograms were obtained. During the electrochemical cleaning process, variation of XPS survey spectra and voltammograms are shown in Fig. S6b-S6d. .

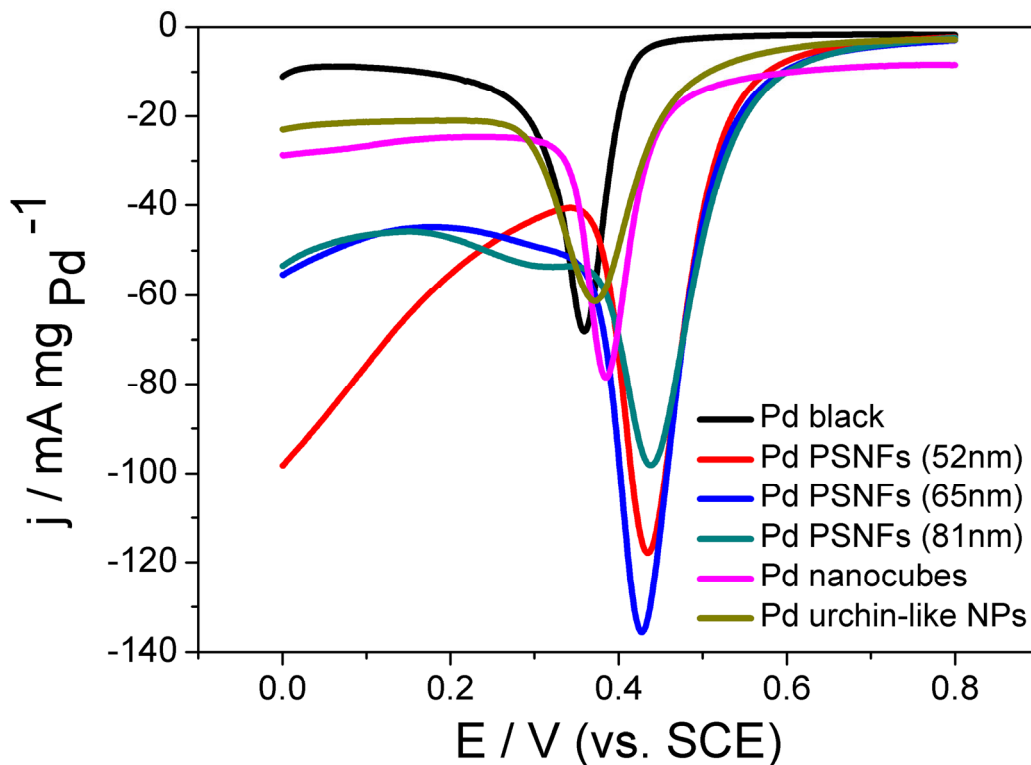


Fig. S7 Cyclic voltammograms recorded at the scan rate of 50 mV s^{-1} in N_2 saturated $0.5 \text{ M H}_2\text{SO}_4$ for the calculation of mass electrochemical active area (ECSA) of the catalysts.

The pattern shows the reduction peak of the oxide of palladium; which indicates the mass ECSA of the catalysts. The detail parameters are summarized in Table 1.

According to the literature, the ECSA of Pd can be obtained from the electric charges for oxygen desorption in palladium oxide during the negative scan.² ECSA were estimated by the following equation:

$$\text{ECSA} = Q_o/q_o,$$

where Q_o is the surface charge that can be obtained from the area under the cyclic voltammetry scanning for oxygen desorption (0–0.8 V) and q_o is the charge required for desorption of monolayer of oxygen on the Pd surface ($424 \mu\text{C cm}^{-2}$)

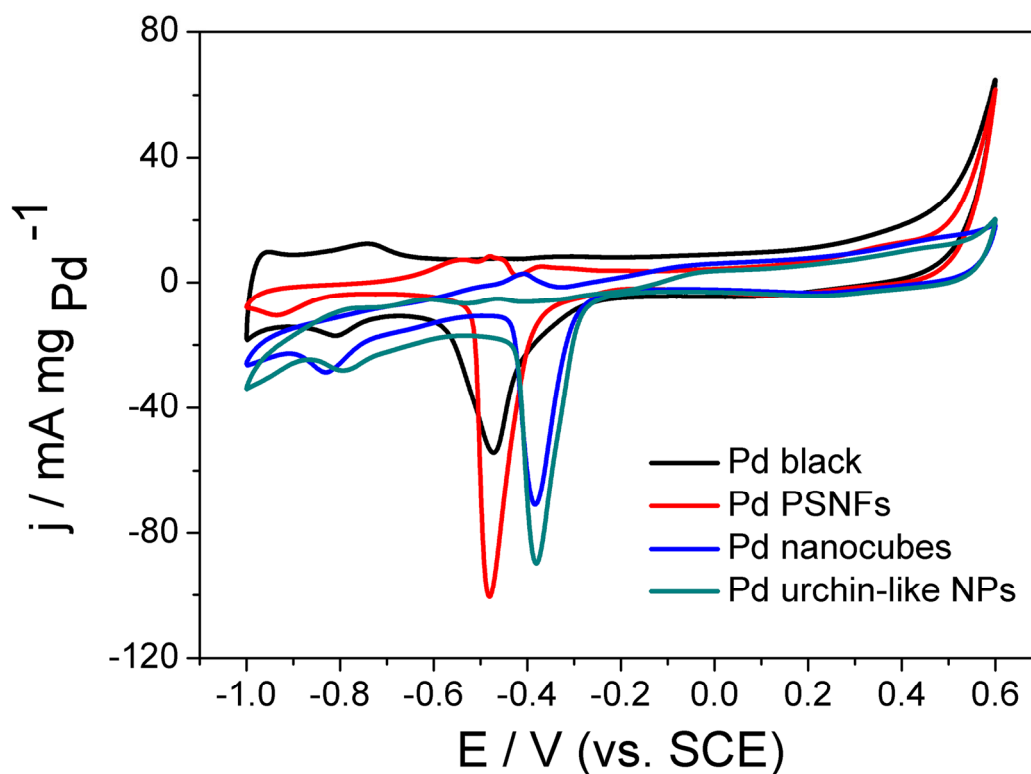


Fig. S8 Blank cyclic voltammograms of four kinds of Pd-based catalysts recorded at room temperature in a solution 1 M KOH (aq) without ethanol with a sweep rate of 50 mV s^{-1} .

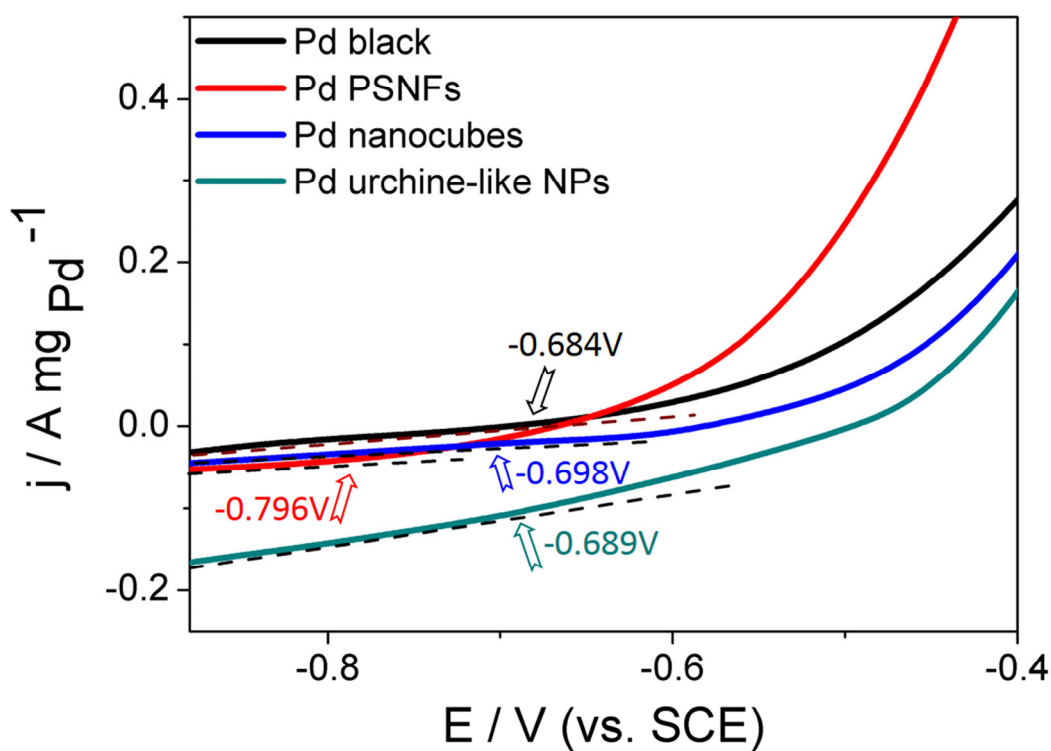


Fig. S9 Amplified area of positive scanning in Fig. 8a to distinguish the onset-potential of four kinds of Pd-based catalysts.

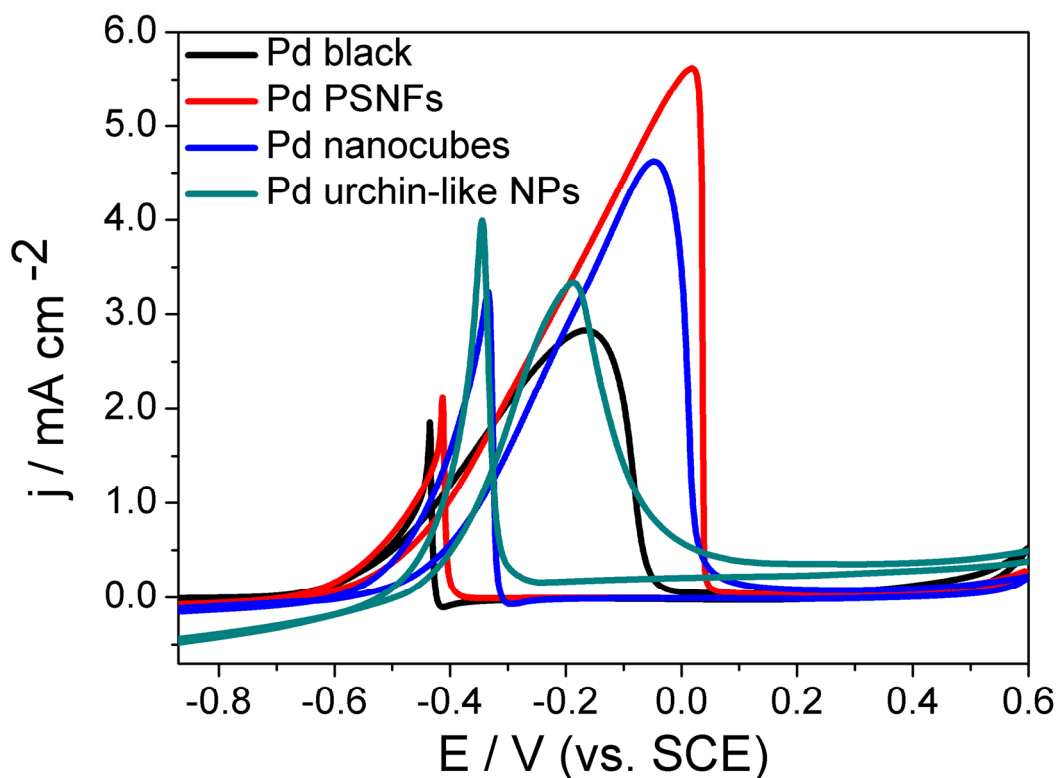


Fig. S10 Specific activity of four kinds of Pd-based catalysts recorded at room temperature in a solution containing 1 M ethanol and 1 M KOH (aq) with a sweep rate of 50 mV s⁻¹.

The results show that Pd PSNFs and Pd nanocubes with enriched {100} facets own a higher EOR activity than {111} facets dominated Pd black and Pd urchin-like nanoparticles, because of the higher EOR activity of Pd {100} facets than Pd {111} facets. Pd PSNFs have plentiful high index facet which is more active than low index facets, thus Pd PSNFs exhibit a better EOR activity than Pd nanocubes as well.

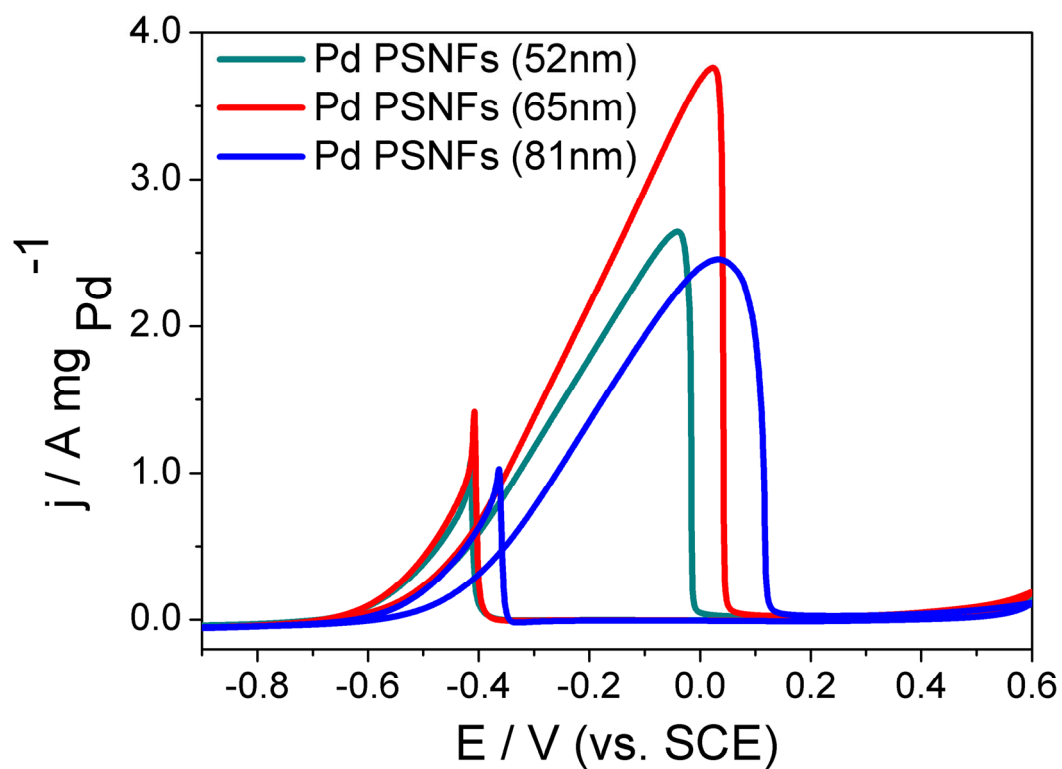


Fig. S11 Cyclic voltammograms of three different size Pd PSNFs recorded at room temperature in a N_2 saturated solution containing 1 M ethanol and 1 M KOH (aq) with a sweep rate of 50 mV s^{-1} , the current density was normalized against the corresponding mass of Pd on each electrode.

Table S1. ICP-MS data for the different size Pd PSNFs, Pd nanocubes and Pd urchin-like NPs.

Catalyst	Measured mass of Pd [μg]	Calculated mass of Pd [μg]	Yield [%]
Pd PSNFs (81nm)	265.49	236.79	89.19
Pd PSNFs (65nm)	278.77	236.51	84.84
Pd PSNFs (52nm)	291.54	250.66	85.98
Pd nanocubes (65nm)	557.52	485.21	87.03
Pd urchin-like NPs (69nm)	278.77	229.34	82.27
Pd black	—	—	—

Table S2. The mass loading, geometric area, active surface area and roughness of the Pd-based catalysts modified FTO electrodes in EOR.

Catalyst	Mass loading [μg]	Geometric area [cm^2]	Active surface area [cm^2]	Roughness ^{a)}
Pd PSNFs (81nm)	15.79	3.00	7.51	2.50
Pd PSNFs (65nm)	15.77	3.00	10.56	3.52
Pd PSNFs (52nm)	16.71	3.00	10.28	3.42
Pd nanocubes (65nm)	32.35	3.00	5.86	1.95
Pd urchin-like NPs (69nm)	15.29	3.00	5.20	1.73
Pd black	15.27	3.00	5.38	1.79

^{a)} Roughness = Active surface area/Geometric area.³

Reference:

1. a) X. Huang, H. Zhang, C. Guo, Z. Zhou, N. Zheng, *Angew. Chem. Int. Ed.* 2009, 48, 4808-4812; b) C. L. Li, M. Imura, Y. Yamauchi, *Phys. Chem. Chem. Phys.* 2014, 16, 8787-8790.
2. a) L. Shi, A. Wang, T. Zhang, B. Zhang, D. Su, H. Li, Y. Song, *J. Phys. Chem. C* 2013, 117, 12526-12536; b) Y. W. Lee, M. Kim, Y. Kim, S. W. Kang, J.-H. Lee, S. W. Han, *J. Phys. Chem. C* 2010, 114, 7689-7693; c) G. Li, L. Jiang, Q. Jiang, S. Wang, G. Sun, *Electrochim. Acta.* 2011, 56, 7703-7711; d) X. Wang, J. Yang, H. Yin, R. Song, Z. Tang, *Adv. Mater.* 2013, 25, 2728-2732.
3. L. Ma, C. Wang, M. Gong, L. Liao, R. Long, J. Wang, D. Wu, W. Zhong, M. J. Kim, Y. Chen, Y. Xie, Y. Xiong, *ACS Nano* 2012, 6, 9797-9806.